crystals

MDPI

Article

Creep Behavior of Squeeze-Cast Mg–15Gd Alloy

Ferdinand Dobeš * and Petr Dymáček

Institute of Physics of Materials, Czech Academy of Sciences, Žižkova 22, CZ-61662 Brno, Czech Republic
* Correspondence: dobes@ipm.cz

Abstract: The creep behavior of a binary Mg-15 wt.% Gd alloy was investigated over the temperature range from 523 K to 743 K, i.e., in both the single-phase region (the hexagonal close-packed solid solution of Gd in Mg) and the two-phase region (the solid solution plus Mg_5Gd precipitates). The alloy was prepared by the squeeze casting technique. In the higher temperature range, at 723 and 743 K, the specimens were solution treated by in situ annealing prior to testing. At the temperature of 673 K and below, the alloy was tested in the cast state. In the higher temperature range, the behavior was interpreted in terms of the viscous glide, where the dislocation motion was constrained by the presence of solute atmospheres. The dislocation motion was controlled by the rate of the cross slip from the basal to the prismatic planes. At the temperatures of 623 K and 673 K, the creep behavior was rationalized by introducing the threshold stress concept. At the temperatures of 523 K and 573 K, the stresses required to achieve experimentally measurable creep rates were such that dislocations broke away from the atmospheres of foreign atoms. Comparison with a series of magnesium alloys prepared by squeeze casting and creep-tested by the same technique showed that gadolinium can be a favorable creep-resistance enhancing element.

Keywords: creep; magnesium alloy; gadolinium; squeeze casting; threshold stress

check for updates

Citation: Dobeš, F.; Dymáček, P. Creep Behavior of Squeeze-Cast Mg–15Gd Alloy. *Crystals* **2023**, *13*, 374. https://doi.org/10.3390/cryst13030374

Academic Editors: Li-Wei Tseng, Yu-Chih Tzeng and Yeong-Lin Lai

Received: 7 February 2023
Revised: 16 February 2023
Accepted: 20 February 2023
Published: 22 February 2023

1. Introduction

Lightweight Mg-based alloys are attractive structural materials for a wide range of applications in modern industry. In many cases, it is necessary to improve their mechanical, corrosion, and physical properties by alloying. Suitable additives are rare earth (RE) metals. Their addition can significantly improve the high-temperature strength and creep resistance. The effect on the drop in the transition temperature between brittle and ductile behavior is also not negligible. As a result, RE additions are primarily intended to improve the performance and safety in the most demanding situations. Such situations occur in space, aerospace, and ground transportation. Examples of various applications for aircraft and missile components are given in Ref. [1]. The alloying by the RE elements for possible biomedical applications is discussed in Ref. [2].

Increasing the creep resistance of magnesium alloys is an extremely important task in terms of the potential of these alloys in a number of applications [3,4]. The addition of cerium (as a major component of mischmetal) to Mg-Al-based alloys enabled the development of AE series commercial alloys followed by the combination of rare earths and zinc (ZE series), silver (QE series), and yttrium (YE series) [1]. The progress in the commercial production of rare earth metals and thus the easier availability of other elements from this group has contributed to the expansion of the spectrum of alloying additives, such as neodymium [5,6], erbium [7], dysprosium [8] or ytterbium [9]. In terms of their application at elevated temperatures, the creep of squeeze-cast magnesium–scandium binary alloys was studied [10]. High-pressure die-cast Mg-Al-La alloys were developed with a similar intention [11]. Abnormal stress exponents in the creep of high-pressure die-cast Mg-Al-RE alloys were rationalized by simultaneously introducing a threshold stress and an internal stress [12].

In recent years, increased attention has been paid to alloys with gadolinium [13,14].

Gadolinium is an effective solid solution strengthener of magnesium due to the misfit atom size and the valence factor [15]. Ultra-high strength was achieved in a simple binary Mg-13Gd alloy by hot extrusion with low plastic deformation and subsequent aging [16]. A high-strength Mg–11Gd–2Ag alloy sheet with extra-low anisotropy was prepared by a combination of rolling and aging [17]. The use of Mg-Gd-based alloys in many medical applications is very promising due to their good biocompatibility and biodegradability [18–20]. For potential application at elevated temperatures, magnesium alloys with gadolinium contents greater than 8–10% (weight percent is given throughout) have been supplemented with yttrium (to reduce the toughness and cost problems), zinc and/or calcium (to enhance the age hardening response and the creep strength), and zirconium (to refine the grain size) [21–29].

For binary alloys with a gadolinium content of more than 10%, there are several pioneering reports in the literature that also presented the results of creep tests, in some cases up to the temperature of 623 K [30–32]. The purpose of these reports was to provide a rough classification of such alloys in terms of creep resistance, rather than to identify deformation controlling processes. An important deformation parameter, the strain rate sensitivity index, was estimated up to the temperature of 573 K for the dilute Mg-Gd alloy [33]. Works studying the creep of magnesium alloys with gadolinium over a wider range of stress or temperature have only recently been published [34–37]. However, even in these recent works, temperatures above 573 K were not studied.

To fully exploit the potential of magnesium alloys with gadolinium additions, it is necessary to have detailed knowledge of the mechanisms by which creep deformation takes place under the widest possible range of conditions. The purpose of the present paper is to investigate the creep behavior of the squeeze-cast binary alloy Mg-15Gd at temperatures above the temperature of the usual T6 peak-aging treatment up to the temperatures of the existence of the single-phase solid solution.

2. Materials and Methods

2.1. Experimental Alloy

The binary Mg-15Gd alloy used in this study was supplied by the Materials Science and Engineering Werkstoffzentrum Clausthal GmbH, Clausthal-Zellerfeld, Germany, in the form of a cast block of dimensions 10 * 10 * 6 cm^3. The alloy was produced by squeeze casting under a protective gas atmosphere (Ar + 1% SF_6). The melting temperature was 1023 K, and the die temperature was 473 K. The actual gadolinium concentration was 14.6 wt.% (2.57 at.%), as determined by atomic absorption spectroscopy with an accuracy of 0.1%.

2.2. Microscopic Observations

To analyze the microstructure, the specimens were mechanically ground up to 2500 SiC paper, mechanically polished (3 µm and 1 µm diamond paste, 5 min each step), and finished with oxide polishing suspension (OPS) (Struers, Ballerup, Denmark). An inverted optical microscope Olympus GX51 (Olympus Corporation, Shinjuku, Japan) was used for the characterization of the micrographs.

The microstructure of the present alloy was described in detail in a previous paper [38]. The microstructure has features typical of cast materials. It consists of primary solidified dendrites and an interdendritic eutectic enriched in gadolinium. According to the transmission electron observations, stable β phase particles (Mg_5Gd, face centered cubic) gradually precipitate from the supersaturated solid solution through the metastable phases β″ (D019) and β′ (c-base centered orthorhombic) [38]. The cast microstructure is retained even after creep for 1060 h at 523 K, see Figure 1.

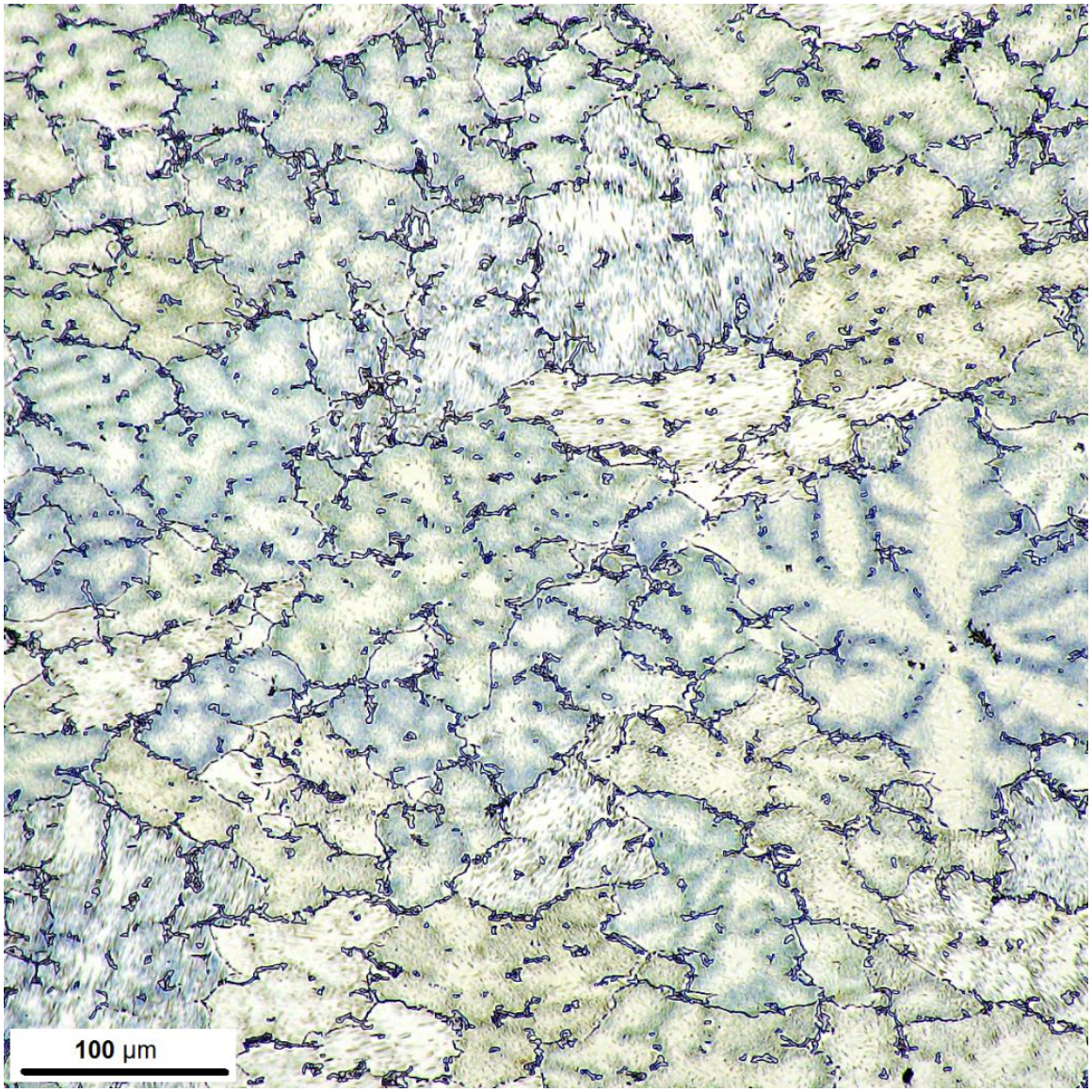

Figure 1. Optical micrograph showing the microstructure after creep at 523 K for 1060 h.

2.3. Creep Tests

Creep tests were performed in uniaxial compression on specimens with a gauge length of 12 mm and a diameter of 8 mm. The specimens were prepared by traveling wire electro-discharge machining and the fine grinding of contact surfaces. The tests were performed on a dead-weight creep machine that was constructed in-house in a protective atmosphere of dry purified argon [39]. The compressive testing allows studying the creep deformation not affected by the onset of fracture processes. The technique was described in more detail in our previous paper [40]. Examples of the time dependence of the true compressive strain are given in Figure 2.

It follows from the Mg-Gd binary phase diagram [41] that in the studied temperature range (i.e., from 523 K to 743 K) the alloy extended into two phase fields: above the temperature of 713 K, a single phase solid solution existed, whereas at temperatures below 713 K the alloy in equilibrium consisted of a solid solution matrix and Mg_5Gd precipitates. In view of these two different situations, different test regimes were chosen. (i) At 723 K and 743 K, the specimens were held in the creep apparatus at the test temperature for 24 h prior to loading to ensure that the alloy was indeed in a single phase state. The temperatures were chosen so that the tests were carried out with sufficient certainty in this region and so

the sample was not threatened by an overshoot above the eutectic temperature when heated to the test temperature. (ii) In the two-phase region, the test temperatures were above the T6 peak-aging temperature up to a temperature that was still safely in this region and with a division of 50 K. The specimens were kept at the test temperature only for the time necessary to stabilize the temperature. Therefore, the specimens were intentionally tested in the as-cast condition. This best corresponds to a situation where die castings are used in conditions of elevated temperatures. For comparison, some specimens at the temperature of 673 K were tested after initial in situ annealing for 24 h at the test temperature, as in the single phase range (i) described above. The differences between the test results with and without the initial annealing were negligible.

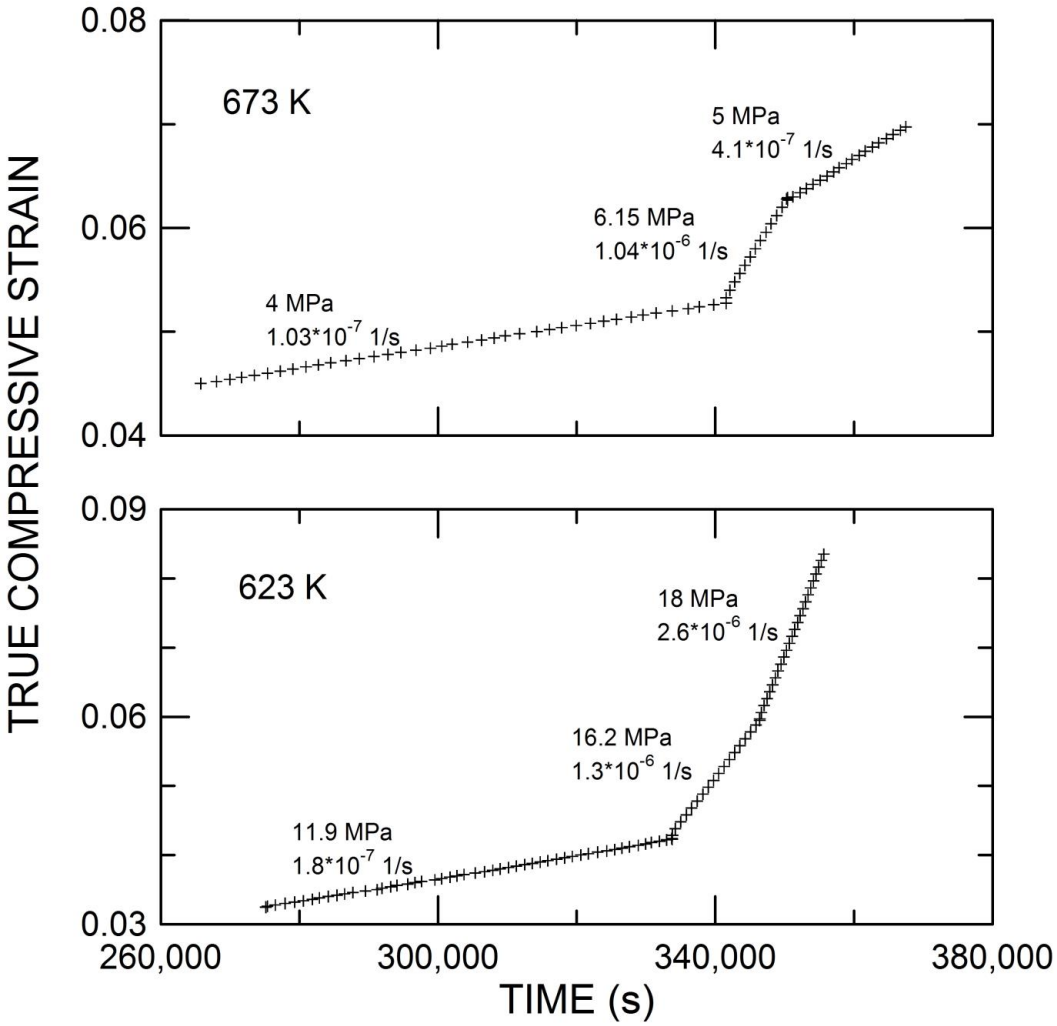

Figure 2. Examples of creep curves at 623 K and 673 K. The true compressive stress and the true compressive strain rate are given for each segment.

2.4. Creep Data Analysis

The dependence of the creep rate on the applied stress σ at a given absolute temperature T was analyzed using the combination of power law and the Arrhenius equation [42]

$$\dot{\varepsilon} = A\sigma^n exp\left(\frac{-Q}{RT}\right), \quad (1)$$

where A is a material constant, n is the stress exponent, Q is the apparent activation energy of creep, and R is the universal gas constant. The values of n and Q can be found as partial derivatives of this equation

$$n = \left(\frac{\partial \ln \dot{\varepsilon}}{\partial \ln \sigma}\right)_T, \quad (2)$$

$$Q = -\left(\frac{\partial \ln \dot{\varepsilon}}{\partial \frac{1}{RT}}\right)_\sigma. \quad (3)$$

3. Results

The creep rates $\dot{\varepsilon}$ measured at different temperatures T were plotted against the applied stress σ in double logarithmic coordinates, as shown in Figure 3. The creep rate increased with both stress and temperature. At high temperatures, i.e., in the region where the existence of a solid solution can be assumed in accordance with the binary phase diagram, the values of n and Q were determined by multiple linear regression: n = 3.17, Q = 164 kJ/mol. At lower temperatures, i.e., in the two-phase region, the stress exponent n was determined separately for each temperature. The stress exponent n corresponded to the slope of the dependences at a constant temperature. From the results shown in Figure 4, it is clear that n was temperature dependent in this region. The activation energy was proportional to the distance between the individual temperatures in Figure 3 at the same stress. The estimated approximate values increased with the increasing applied stress to a value of about 370 kJ/mol at 50 MPa and then decreased with the increasing stress, see Figure 5. The values were significantly higher than any enthalpy of lattice diffusion that could be considered for this alloy. However, it should be emphasized that this was the apparent activation energy. The effective values of the activation energy are discussed in the next section.

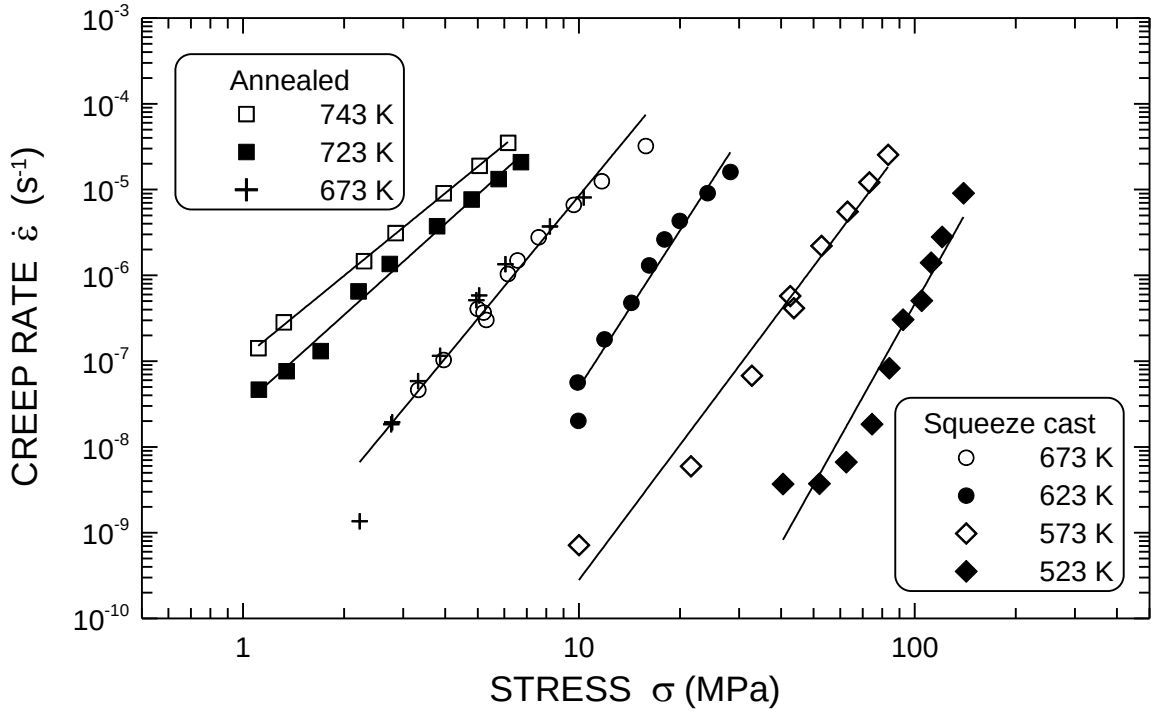

Figure 3. Dependence of the creep rate on the applied stress at different temperatures.

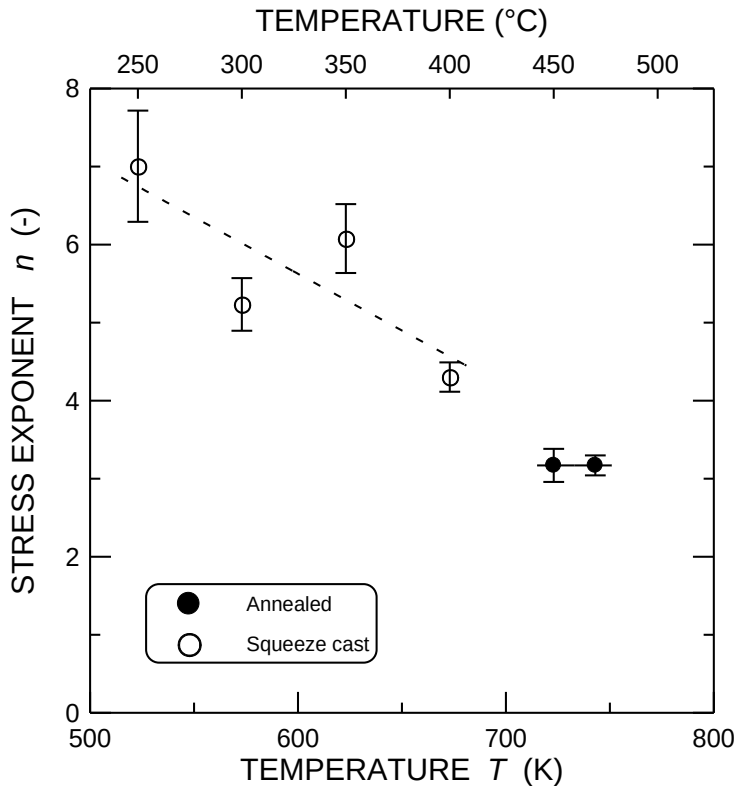

Figure 4. Variation of the stress exponent of the creep rate with temperature.

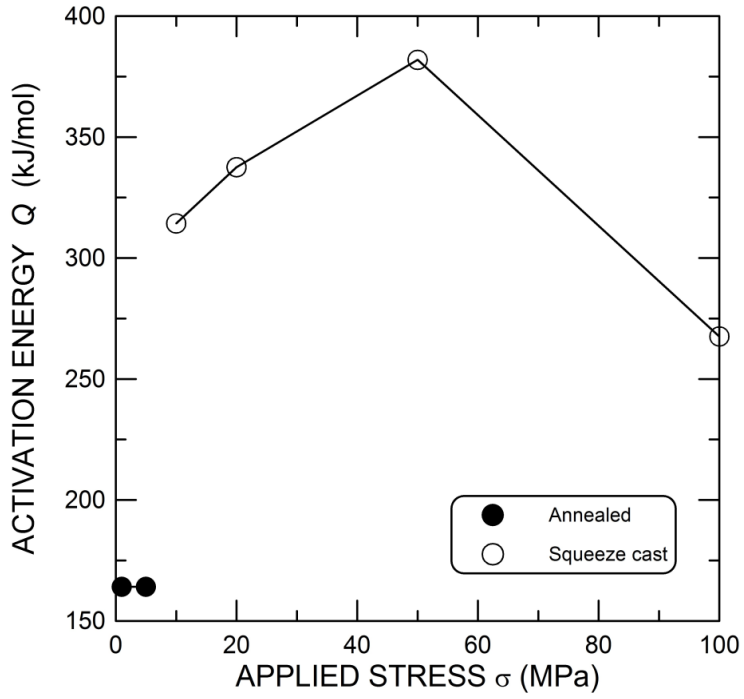

Figure 5. The values of the apparent activation energy estimated for various applied stresses.

4. Discussion

4.1. Single Phase Region

The deformation mechanism characterized by a similar value of the stress exponent, i.e., $n = 3$, is usually described as the viscous motion of dislocations [42]. In this mechanism, the deformation is governed by the glide of the dislocations, which drag the atmosphere of solute atoms. Another characteristic feature of the creep controlled by the viscous motion

of the dislocations should be the proximity of the activation energy of the creep and the activation enthalpy of the diffusion of the solute atoms. The diffusion coefficient can be taken as that of the chemical interdiffusivity suggested either by Darken [43] or by Fuentes-Samaniego et al. [44,45] and given by a combination of the tracer diffusion coefficients for the solvent and solute atoms in the alloy. The activation enthalpy of the diffusion of Gd in magnesium was recently determined to be 128.4 kJ/mol [46]. The traditionally accepted value of the activation enthalpy of the lattice diffusion of magnesium, 135 kJ/mol [47], was close to the value of 138.44 kJ/mol used by Zhong et al. [46]. In this range, i.e., between 128 and 138 kJ/mol, the activation enthalpy of the chemical interdiffusion in the studied alloy can also be expected.

Good agreement between the activation energy of the steady-state creep rate and that of the self-diffusion has been shown for a number of materials. One exception is the creep of hexagonal metals at high homologous temperatures with anomalously high activation energy [48]. We illustrate this phenomenon by means of the activation energies reported by Vagarali and Langdon for pure Mg [49] and a Mg-Al solid solution [50]. The detected creep activation energy clearly corresponded well to the values found by Vagarali and Langdon for pure magnesium (Figure 6). It should be noted that Vagarali and Langdon used a slightly different method to determine the activation energy of the creep, which included the temperature dependence of the modulus of elasticity, $G = (1.92 * 10^4 - 8.6 * T)$ MPa,

$$Q = -\frac{\partial \ln\left(\dot{\varepsilon} G^{n-1} T\right)}{\partial\left(\frac{1}{RT}\right)}. \quad (4)$$

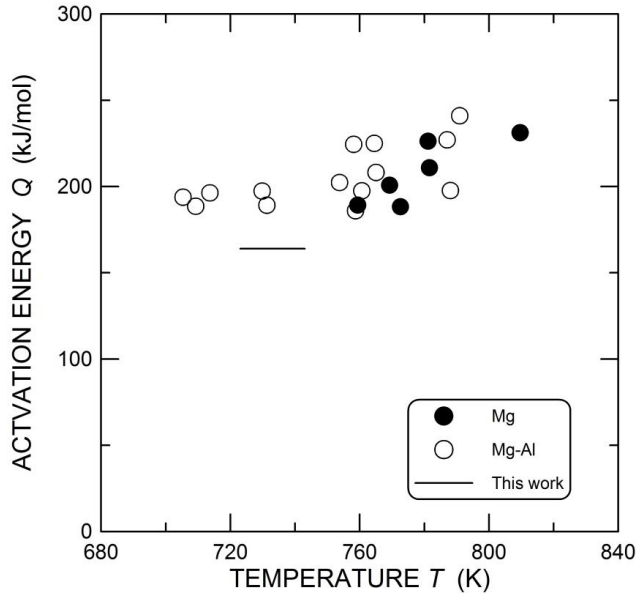

Figure 6. Comparison of the activation energies of the creep at high temperatures in pure magnesium [49], Mg-0.8% Al [50], and in the present alloy.

The difference between the results of the two methods was minimal; our procedure gave a value approximately 0.4 kJ/mol higher. The similarity of the presented values of the stress exponent and the activation energy with the values found by Vagarali and Langdon allows us to consider the same deformation mechanism, controlled by the rate of cross-slip from the basal to the prismatic planes even in the case of the Mg-Gd solid solution.

4.2. Two Phase Region

In accordance with the phase diagram, particles of the secondary phase Mg_5Gd precipitated in the studied alloy at temperatures below T = 713 K [41]. Their presence impeded the movement of the dislocations, and the creep rate was then proportional to

the effective stress, which is given by the difference between the applied stress σ and the threshold stress σ_0 delineating a lower limiting stress for any measurable flow [51]

$$\dot{\varepsilon} \propto (\sigma - \sigma_0)^n. \quad (5)$$

If the effective stress is close to the stresses occurring during the creep in the region of the solid solution, the power n should have a similar value, i.e., $n = 3$. The value of the threshold stress σ_0 can be determined by plotting $\dot{\varepsilon}^{1/3}$ against the applied stress on the linear axes and extrapolating linearly to a zero creep rate. The procedure is illustrated in Figure 7. The resulting threshold stress was temperature dependent: at 673 K, it was equal to 1.87 MPa, and at 623 K, it was 7.27 MPa. The activation energy of the creep must be determined in this temperature range at a constant effective stress, $(\sigma - \sigma_0)$, see Figure 8. The resulting value was 133.8 kJ/mol; the value determined by the abovementioned Vagarali and Langdon [49] method was approximately 0.8 kJ/mol higher. In this interval of reduced temperatures, the cross slip of the dislocations to the prismatic planes no longer took place, and the activation energy of the creep was close to the activation enthalpy of the interdiffusion. Given the values of the effective stress power and activation energy, it is reasonable to conclude that the creep was controlled by the viscous glide of the dislocations.

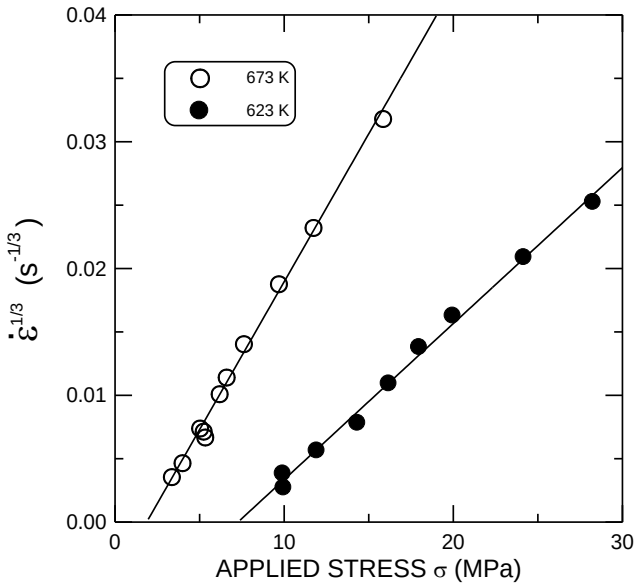

Figure 7. The relationship between $\dot{\varepsilon}^{1/3}$ and the applied stress in the double linear coordinates.

From the experimental data at temperatures of 573 K and 523 K, it was difficult to evaluate an acceptable threshold stress. This situation can be caused by a change in the mechanism of the dislocation motion. At increased stress, dislocations break away from the cloud of foreign atoms and their motion is characterized by higher stress sensitivity. The critical break stress is given by [52]

$$\sigma_B = \left(\frac{1}{2\pi}\right)^2 \left(\frac{1+\nu}{1-\nu}\right)^2 \frac{MG^2 c\Delta V^2}{10b^3 kT}, \quad (6)$$

where ν is the Poisson ratio, $M = 3.06$ is the Taylor factor, c is the concentration of the solute atoms, $\Delta V = 9.85 * 10^{-30}$ m^3 is the difference in volume between the solute and solvent atoms, and $b = 3.2 * 10^{-10}$ m is the length of Burgers vector. The hatched area in Figure 9 represents the values of the break stress calculated using Equation (6). For the left-hand boundary, the gadolinium concentrations in solid solution according to the equilibrium phase diagram were used. The right-hand limit corresponded to the maximum concentration of gadolinium in the alloy studied, i.e., 2.57 at.%. For the equilibrium

concentrations, i.e., c = 0.0053 at 523 K and c = 0.0088 at 573 K [41], we obtained the break stress of 14.8 MPa and 21.3 MPa at the respective temperatures. Thus, when compared with the results of the creep tests, it was clear that at 523 K, the creep would take place completely above the break stress and at 573 K for the most part. On the other hand, at a temperature of 623 K and the corresponding equilibrium gadolinium concentration of 0.0137, the break stress was 28.5 MPa. The extrapolation to zero creep rate in the determination of the threshold stress (see Figure 7) was not affected by any change in the deformation mechanism at this temperature and was therefore justified.

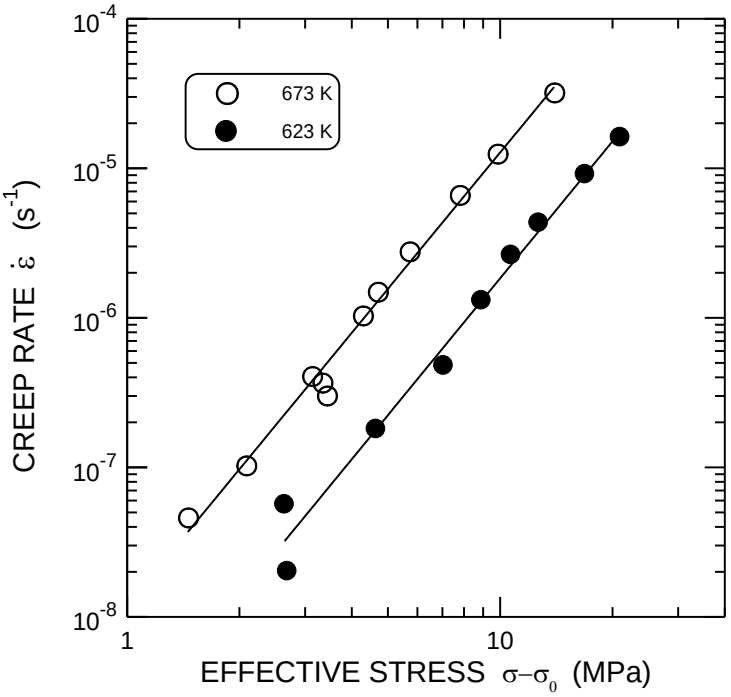

Figure 8. The relation between the creep rate and the effective stress in the double logarithmic coordinates.

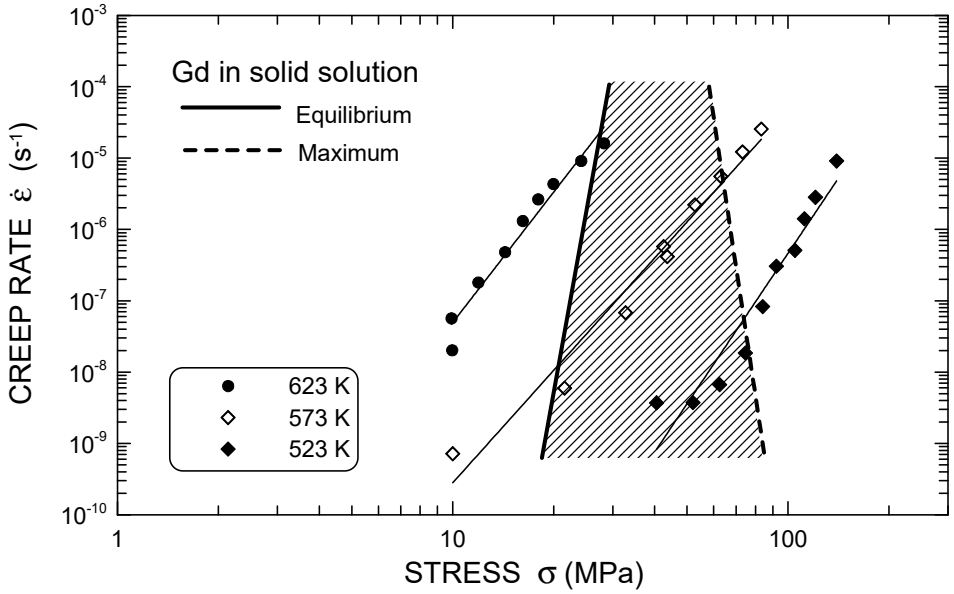

Figure 9. The creep rate vs. the applied stress for the three temperatures in the two phase region: the hatched quadrangle indicates the onset of the dislocation breaking from the gadolinium atoms.

4.3. Comparison with Cast Pure Magnesium and Squeeze-Cast Magnesium Alloys

In the next part, we attempt to compare our binary alloy with various magnesium alloys produced by the same technology, i.e., squeeze casting, and previously tested in the same way in the same creep laboratory. In addition to alloys where aluminum alloying was combined with zinc, silicon, or strontium, rare earth-alloyed alloys were also included in this rather random selection. These alloys were: AS21 (2.2 Al, 1.0 Si, 0.1 Mn), AZ91 (9.0 Al, 0.7 Zn, 0.3 Mn), QE22 (2.2 Ag, 2.1 Dy), ZE41 (4.2 Zn, 1.2 RE, 0.7 Zr) [53], and AJ62 (6 Al, 2 Sr) [54]. The results are summarized in Figure 10. For completeness, the results of the compressive creep tests of the cast pure magnesium are also given [53]. It is clear that the creep resistance of the present simple binary alloy was superior to that of the other tested squeeze-cast magnesium alloys. From the above results, it can be concluded that gadolinium can be a favorable creep-resistance enhancing element, especially in the two-phase region, where the dislocation motion is impeded by the presence of the intermetallic phase Mg_5Gd.

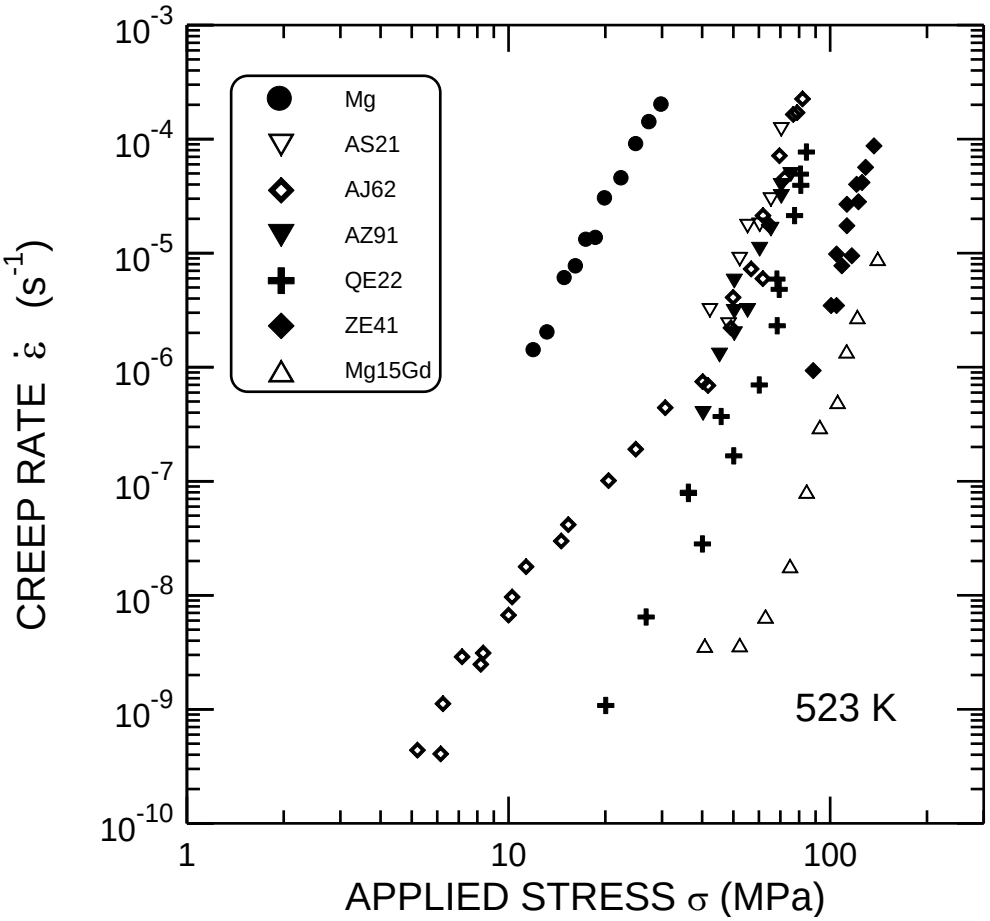

Figure 10. Comparison of the creep behavior at 523 K of the present binary alloy, pure magnesium [53], AJ62 alloy [54] and some squeeze-cast magnesium alloys [53] tested in uniaxial compression.

5. Conclusions

In this work, compressive creep tests were conducted on a binary Mg-Gd alloy with 15 wt.% gadolinium prepared by the squeeze casting technique. Creep tests were performed in the temperature range from 523 K to 743 K. The mechanisms of the plastic deformation were identified, probably for the first time, over the entire temperature range. This is important both from the point of view of determining the creep resistance and for optimizing the technological processes during formation at elevated temperatures. The results are summarized as follows:

- In the higher temperature range, the activation energy of the creep was 164 kJ/mol, and the stress exponent was n = 3.17. The behavior was interpreted in terms of the viscous glide, where the dislocation motion was constrained by the presence of the solute atmospheres. The dislocation motion was controlled by the rate of cross-slip from the basal to the prismatic planes.
- The fact that the activation energy was higher than the activation enthalpy of diffusion must be considered when predicting heat resistance, which is usually based on experiments at higher temperatures due to time constraints.
- At temperatures of 623 K and 673K, the creep behavior was rationalized by introducing the threshold stress concept. The value of the stress exponent found in the single-phase region was used to determine the threshold stress in the two-phase region. To the best of the authors' knowledge, this procedure has not been used in the creep analysis of magnesium alloys. The dislocation velocity was still limited by the solute atoms, but the cross slip to the prismatic planes no longer played a significant role due to the reduced temperature.
- At temperatures of 523 K and 573 K, the stresses required to achieve experimentally measurable creep rates were so large that the dislocations broke away from the atmospheres of the foreign atoms.
- At temperatures lower than those studied in this work, it would be interesting to study the critical stress for the dislocation detachment from the solute atmospheres in a material that has undergone hardening annealing. This study may lead to the optimization of the heat treatment.
- Comparison with a series of magnesium alloys prepared by squeeze casting and tested by the same technique showed that gadolinium can be a favorable creep-resistance enhancing element.

Author Contributions: F.D.: performed the creep tests and all calculations and wrote the paper; P.D.: conceived the research, prepared the experimental specimens, performed the microstructural observations, and edited the text. All authors have read and agreed to the published version of the manuscript.

Funding: This research received no external funding.

Data Availability Statement: The data presented in this study are available on request from the corresponding author. The data are not publicly available due to ongoing research.

Acknowledgments: The authors thank Sebastian Cramer from Materials Science and Engineering Werkstoffzentrum Clausthal GmbH for providing squeeze casting details.

Conflicts of Interest: The authors declare no conflict of interest.

References

1. Rokhlin, L.L. *Magnesium Alloys Containing Rare Earth Metals*; Taylor & Francis: London, UK, 2003.
2. Dong, J.; Lin, T.; Shao, H.; Wang, H.; Wang, X.; Song, K.; Li, Q. Advances in degradation behavior of biomedical magnesium alloys: A review. *J. Alloys Compd.* **2022**, *908*, 164600. [CrossRef]
3. Pekguleryuz, M.; Celikin, M. Creep resistance in magnesium alloys. *Inter. Mater. Rev.* **2010**, *55*, 197–217. [CrossRef]
4. Mo, N.; Tan, Q.; Bermingham, M.; Huang, Y.; Dieringa, H.; Hort, N.; Zhang, M.-X. Current development of creep-resistant magnesium cast alloys: A review. *Mater. Des.* **2018**, *155*, 422–442. [CrossRef]
5. Chia, T.L.; Easton, M.A.; Zhu, S.M.; Gibson, M.A.; Birbilis, N.; Nie, J.F. The effect of alloy composition on the microstructure and tensile properties of binary Mg-rare earth alloys. *Intermetallics* **2009**, *17*, 481–490. [CrossRef]
6. Yan, J.; Sun, Y.; Xue, F.; Xue, S.; Tao, W. Microstructure and mechanical properties in cast magnesium–neodymium binary alloys. *Mater. Sci. Eng.* **2008**, *A476*, 366–371. [CrossRef]
7. Wu, B.L.; Wan, G.; Du, X.H.; Zhang, Y.D.; Wagner, F.; Esling, C. The quasi-static mechanical properties of extruded binary Mg–Er alloys. *Mater. Sci. Eng.* **2013**, *A573*, 205–214. [CrossRef]
8. Yang, L.; Huang, Y.; Peng, Q.; Feyerabend, F.; Kainer, K.U.; Willumeit, R.; Hort, N. Mechanical and corrosion properties of binary Mg–Dy alloys for medical applications. *Mater. Sci. Eng.* **2011**, *B176*, 1827–1834. [CrossRef]
9. Wu, H.; Yan, T.; Wang, L.; Li, X.; Wei, Y.; Li, S.; Wang, X.; Wu, R. Effect of Yb addition on the microstructure and mechanical properties of ZK60 alloy during extrusion. *Mater. Sci. Eng.* **2020**, *A777*, 139033. [CrossRef]

10. Mordike, B.L.; Stulíková, I.; Smola, B. Mechanisms of creep deformation in Mg-Sc–based alloys. *Metal. Mater. Trans.* **2005**, *A36*, 1729–1736. [CrossRef]
11. Zhang, J.; Liu, S.; Leng, Z.; Liu, X.; Niu, Z.; Zhang, M.; Wu, R. Structure stability and mechanical properties of high-pressure die-cast Mg–Al–La–Y-based alloy. *Mater. Sci. Eng.* **2012**, *A531*, 70–75. [CrossRef]
12. Yang, Q.; Yan, Z.; Lv, S.; Guan, K.; Qiu, X. Abnormal creep stress exponents in a high-pressure die casting Mg–Al−RE alloy. *Mater. Sci. Eng.* **2022**, *A831*, 142203. [CrossRef]
13. Zhang, J.; Liu, S.; Wu, R.; Hou, L.; Zhang, M. Recent developments in high-strength Mg-RE-based alloys: Focusing on Mg-Gd and Mg-Y systems. *J. Magnes. Alloys* **2018**, *6*, 277–291. [CrossRef]
14. Liu, J.; Sun, J.; Chen, Q.; Lu, L.; Zhao, Y. Study on Microstructure and Mechanical Property in Mg-Gd-Y Alloy by Secondary Extrusion Process. *Crystals* **2021**, *11*, 939. [CrossRef]
15. Gao, L.; Chen, R.S.; Han, E.H. Effects of rare-earth elements Gd and Y on the solid solution strengthening of Mg alloys. *J. Alloys Compd.* **2009**, *481*, 379–384. [CrossRef]
16. Li, R.G.; Li, H.R.; Pan, H.C.; Xie, D.S.; Zhang, J.H.; Fang, D.Q.; Dai, Y.D.; Zhao, D.Y.; Zhang, H. Achieving exceptionally high strength in binary Mg-13Gd alloy by strong texture and substantial precipitates. *Scripta Mater.* **2021**, *193*, 142–146. [CrossRef]
17. Yang, Z.Q.; Ma, A.B.; Xu, B.Q.; Jiang, J.H.; Sun, J.P. Development of a high-strength Mg–11Gd–2Ag (wt%) alloy sheet with extra-low anisotropy. *Mater. Sci. Eng.* **2021**, *A811*, 141084. [CrossRef]
18. Yao, H.; Li, H.; Liu, Y.; Shi, H. Enhanced mechanical and corrosion properties of grain refined Mg-2.0Zn-0.5Zr-3.0Gd alloy. *Kovové Mater.* **2020**, *58*, 409–421. [CrossRef]
19. Zheng, X.; Fan, J.; Tan, S.; Zhang, X. Effects of Gd and heat treatments on mechanical properties of Mg-xGd-1Zn-0.4Zr alloys. *Kovové Mater.* **2020**, *58*, 423–432. [CrossRef]
20. He, X.; Li, Y.; Miao, H.; Sun, J.; Ong, M.T.Y.; Zu, H.; Li, W. The Bioactive Mg-Zn-Gd Wire Enhances Musculoskeletal Regeneration: An In Vitro Study. *Crystals* **2022**, *12*, 1287. [CrossRef]
21. Anyanwu, I.A.; Kamado, S.; Kojima, Y. Creep Properties of Mg-Gd-Y-Zr Alloys. *Mater. Trans.* **2001**, *42*, 1212–1218. [CrossRef]
22. Zhu, X.; Wang, J.; Xu, Y.; Wang, R.; Nie, J.; Zhu, L. Microstructure and creep behaviour of Mg-12Gd-3Y-1Zn-0.4Zr alloy. *J. Rare Earths* **2013**, *31*, 186–191. [CrossRef]
23. Wang, H.; Wang, Q.D.; Boehlert, C.J.; Yang, J.; Yin, D.D.; Yuan, J.; Ding, W.J. The impression creep behavior and microstructure evolution of cast and cast-then-extruded Mg–10Gd–3Y–0.5Zr (wt%). *Mater. Sci. Eng.* **2016**, *A649*, 313–324. [CrossRef]
24. Mo, N.; McCarroll, I.; Tan, Q.; Ceguerra, A.; Liu, Y.; Cairney, J.; Dieringa, H.; Huang, Y.; Jiang, B.; Pan, F.; et al. Understanding solid solution strengthening at elevated temperatures in a creep-resistant Mg–Gd–Ca alloy. *Acta Mater.* **2019**, *181*, 185–199. [CrossRef]
25. Liu, W.; Zhou, B.; Wu, G.; Zhang, L.; Peng, X.; Cao, L. High temperature mechanical behavior of low-pressure sand-cast Mg–Gd–Y–Zr magnesium alloy. *J. Magnes. Alloys* **2019**, *7*, 597–604. [CrossRef]
26. Garces, G.; Máthis, K.; Barea, R.; Medina, J.; Pérez, P.; Stark, A.; Schell, N.; Adeva, P. Effect of precipitation in the compressive behavior of high strength Mg-Gd-Y-Zn extruded alloy. *Mater. Sci. Eng.* **2019**, *A768*, 138452. [CrossRef]
27. Li, B.; Zhang, K.; Shi, G.; Li, Y.; Li, X.; Ma, M.; Yuan, J.; Wang, K. Abnormal creep behavior of Mg–12Gd–1MM–0.6Zr (wt.%) alloy at 300 °C. *Mater. Lett.* **2021**, *295*, 129861. [CrossRef]
28. Li, B.; Zhang, K.; Shi, G.; Wang, K.; Li, Y.; Li, X.; Ma, M.; Yuan, J. Microstructure evolution, mechanical properties and creep mechanisms of Mg-12Gd-1MM-0.6Zr (wt%) magnesium alloy. *J. Rare Earths* **2021**, *39*, 600–608. [CrossRef]
29. Zhang, Y.; Liu, Z.; Pang, S.; Meng, T.; Zhi, Y.; Xu, Y.; Xiao, L.; Li, R. Investigation of tensile creep behavior of Mg–Gd–Y–Zr alloy based on creep constitutive model. *Mater. Sci. Eng.* **2021**, *A805*, 140567. [CrossRef]
30. Stulíková, I.; Smola, B.; von Buch, F.; Mordike, B.L. Development of Creep Resistant Mg-Gd-Sc Alloys with Low Sc Content. *Mater. Werkst.* **2001**, *32*, 20–24. [CrossRef]
31. Smola, B.; Stulíková, I.; von Buch, F.; Mordike, B.L. Structural aspects of high performance Mg alloys design. *Mater. Sci. Eng.* **2002**, *A324*, 113–117. [CrossRef]
32. Smola, B.; Stulíková, I.; Pelcová, J.; Mordike, B.L. Significance of stable and metastable phases in high temperature creep resistant magnesium–rare earth base alloys. *J. Alloys Compd.* **2004**, *378*, 196–201. [CrossRef]
33. Stanford, N.; Sabirov, I.; Sha, G.; La Fontaine, A.; Ringer, S.P.; Barnett, M.R. Effect of Al and Gd Solutes on the Strain Rate Sensitivity of Magnesium Alloys. *Metall. Mater. Trans.* **2010**, *A41*, 734–743. [CrossRef]
34. Wang, J.; Luo, L.; Huo, Q.; Shi, Y.; Xiao, Z.; Ye, Y.; Yang, X. Creep behaviors of a highly concentrated Mg-18 wt%Gd binary alloy with and without artificial aging. *J. Alloys Compd.* **2019**, *774*, 1036–1045. [CrossRef]
35. Ouyang, S.; Yang, G.; Qin, H.; Luo, S.; Xiao, L.; Jie, W. High temperature creep behavior and creep microstructure evolution of T6 state Mg–15Gd alloy. *Mater. Sci. Eng.* **2020**, *A780*, 139138. [CrossRef]
36. Chen, C.; Huo, Q.; Zhang, Z.; Zhang, Y.; Tang, J.; Li, K.; Ma, J.; Yang, X. Effects of precipitate origin and precipitate-free zone development on the tensile creep behaviors of a hot-rolled Mg-13wt%Gd binary alloy. *Mater. Char.* **2021**, *178*, 111303. [CrossRef]
37. Ouyang, S.; Yang, G.; Qin, H.; Wang, C.; Luo, S.; Jie, W. Effect of the precipitation state on high temperature tensile and creep behaviors of Mg-15Gd alloy. *J. Magnes. Alloys* **2022**, *10*, 3459–3469. [CrossRef]
38. Vostrý, P.; Smola, B.; Stulíková, I.; von Buch, F.; Mordike, B.L. Microstructure Evolution in Isochronally Heat Treated Mg-Gd Alloys. *Phys. Stat. Sol. (a)* **1999**, *175*, 491–500. [CrossRef]

39. Dobeš, F.; Zvěřina, O.; Čadek, J. Modified lever system for constant-stress compressive creep machine. *J. Test. Eval.* **1986**, *14*, 271–273.
40. Dobeš, F.; Dymáček, P.; Friák, M. Creep of Heusler-Type Alloy Fe-25Al-25Co. *Crystals* **2020**, *10*, 52. [CrossRef]
41. Hampl, M.; Blawert, C.; Silva Campos, M.R.; Hort, N.; Peng, Q.; Kainer, K.U.; Schmid-Fetzer, R. Thermodynamic assessment and experimental study of Mg-Gd alloys. *J. Alloys Compd.* **2013**, *581*, 166–177. [CrossRef]
42. Perez-Prado, M.-T.; Kassner, M.E. The 3-Power-Law Viscous Glide Creep. In *Fundamentals of Creep in Metals and Alloys*, 3rd ed.; Kassner, M.E., Ed.; Butterworth-Heinemann/Elsevier: Oxford, UK, 2015; pp. 129–138. [CrossRef]
43. Darken, L.S. Diffusion, mobility and their interrelation through free energy in binary metallic systems. *Trans. AIME* **1948**, *175*, 184–201.
44. Fuentes-Samaniego, R.; Nix, W.D.; Pound, G.M. Vacancy and substitutional solute distribution around an edge dislocation in equilibrium and in steady-state glide motion. *Philos. Mag.* **1980**, *A42*, 591–600. [CrossRef]
45. Fuentes-Samaniego, R.; Nix, W.D. Appropriate diffusion coefficients for describing creep processes in solid solution alloys. *Scripta Metal.* **1981**, *15*, 15–20. [CrossRef]
46. Zhong, W.; Zhao, J.-C. Measurements of diffusion coefficients of Ce, Gd and Mn in Mg. *Materialia* **2019**, *7*, 100353. [CrossRef]
47. Shewmon, P.G.; Rhines, F.N. Rate of self-diffusion in polycrystalline magnesium. *Trans. AIME J. Met.* **1954**, *6*, 1021–1025. [CrossRef]
48. Frost, H.J.; Ashby, M.F. *Deformation-Mechanism Maps—The Plasticity and Creep of Metals and Ceramics*; Pergamon Press: Oxford, UK, 1982.
49. Vagarali, S.S.; Langdon, T.G. Deformation Mechanisms in H.C.P. Metals at Elevated Temperatures-I. Creep Behavior of Magnesium. *Acta Metal.* **1981**, *29*, 1969–1982. [CrossRef]
50. Vagarali, S.S.; Langdon, T.G. Deformation Mechanisms in H.C.P. Metals at Elevated Temperatures-II. Creep Behavior of a Mg-0.8% Al Solid Solution Alloy. *Acta Metal.* **1982**, *30*, 1157–1170. [CrossRef]
51. Li, Y.; Langdon, T.G. A Unified Interpretation of Threshold Stresses in the Creep and High Strain Rate Superplasticity of Metal Matrix Composites. *Acta Mater.* **1999**, *47*, 3395–3403. [CrossRef]
52. Friedel, J. *Dislocations*; Pergamon Press: Oxford, UK, 1964.
53. Milička, K.; Trojanová, Z.; Lukáč, P. Internal stresses during creep of magnesium alloys at 523 K. *Mater. Sci. Eng.* **2007**, *A462*, 215–219. [CrossRef]
54. Dobeš, F.; Dymáček, P. Creep behavior of AJ62 Magnesium–Aluminum–Strontium alloy. *J. Magnes. Alloys* **2020**, *8*, 414–420. [CrossRef]